Effectiveness of micro synthetic jet actuator enhanced by flow instability

Guang Hong

Faculty of Engineering

University of Technology Sydney (UTS)

PO Box 123, Broadway, NSW 2007, Australia

Email: guang.hong@uts.edu.au

Abstract

This paper aims to understand how a micro synthetic jet actuator works effectively to prevent the boundary layer flow from laminar separation caused by adverse pressure gradient. Experimental results showed that synthetic jets were effective when the forcing frequency was in the range of Tollmien-Schlichting (T-S) waves. They demonstrated the feasibility of controlling a large-scale structure feature, such as flow separation, using a micro actuator which requires very low power supply (±7.5V) and generates inaudible noise in a boundary layer with the Reynolds number of $1.78x10^5$~$2.24x10^5$. The interaction between the synthetic jet and the base flow is analyzed, and the significance of using the instability to make the synthetic jets effective is discussed. To enable a micro actuator to work effectively on preventing the boundary layer flow from laminar separation, the key issue is to use the synthetic jet actuator as an instability trigger to trigger T-S waves which accelerate the viscous transition. The triggered T-S waves are amplified and enhanced by the non-viscous Kelvin-Helmortz (K-H) instability of the base flow and consequently become effective in controlling the K-H instability. As a trigger

rather than a force generator, the synthetic jet actuator actuates independently to its size and weight.

Introduction

Pressure-induced flow separation is a typical phenomenon in the aerodynamic systems, which often causes the increase of drag force and the decrease of energy efficiency. It may appear on small aircrafts like unmanned aerial vehicles (UAVs), on the wings of man-carrying sail planes, on the vanes of turbomachines, on the blades of wind-energy converters, and even on the slats of large commercial jet-powered airlines [18]. Recent research has demonstrated that synthetic jet actuators (SJAs) are very promising devices for active control of flow separation. They are considered as the enabling means for the next-generation of UAVs and advance air mobility systems [17].

A synthetic jet, originated from the idea of acoustic streaming, has been known as a zero-net-mass but non-zero momentum fluid flux generated by a device such as a piezo-oscillator. It has emerged as a versatile actuator with potential applications ranging from separation and turbulence control to thrust vectoring, and augmentation of heat transfer and mixing[4,14,16]. A unique feature of synthetic jets is that they are formed entirely from the working fluid of baseline flow without requirement of additional mass supply [7]. The strong potential of synthetic jet actuators has attracted many researchers in recent years, and representative work includes that reported in [1,2,8,11,14].

Extensive review of work on synthetic jets was provided by [7, 8, 19]. In much of the previous work, the properties of the synthetic jet actuators in a quiescent condition without cross flow were investigated experimentally [7] and numerically [7,15,16]. For synthetic jets in a boundary layer with cross flow, representative work includes using synthetic jets to increase the lifting force, demonstrated in an air flow passing a two-dimensional cylinder or airfoil [1,2,14]. Different devices for active and passive control of gas flows were investigated in NASA Langley Research Center, including passive vortex generators, micro bumps and piezoelectric synthetic jet actuators [13]. The effectiveness of these devices with secondary flows present was evaluated. They concluded that synthetic jet actuators must have sufficient velocity output to provide comparable control.

Characteristic time scale of the actuation is an important issue in terms of control effectiveness, as pointed out by Glezer and Amitay [7]. They drew conclusions on two control approaches emphasizing actuation frequencies. One approach could couple directly the instability mechanisms of the separating layer, but relied on the narrow band receptivity of the separating shear layer to a control input and also on a limited spatial domain within which the control input could be effective. Another approach was to use actuation frequencies higher than the natural vortex shedding frequency. This approach could decouple the global effect from the actuator's forcing frequency. In both approaches, the actuation frequency was determined based on the flow instability.

A micro actuator needs to be not only effective but also efficient. To be efficient, a SJA needs to be driven at the lowest forcing power. In the most recent publication, Gilarranz et al reported their work on developing a high-power synthetic jet actuator which acted as a reciprocating air compressor with a crank system and six pistons[5]. The maximum power consumption of this synthetic jet actuator was 1200W and the peak jet velocity was 124 m/s. They also reported the application of this newly developed synthetic jet actuator to flow separation control over a NACA 0015 wing in conditions with a freestream velocity of 35 m/s and a Reynolds number of 8.96×10^5. Their results showed that the synthetic jet actuation successfully decreased the drag and increased in the maximum lift coefficient by 80% when the angle of attack was varied from 12 to 18 degree[6].

To develop an effective and efficient synthetic jet actuator, issues such as compactness, weight and power density need to be addressed. Addressing these issues requires the understanding of the physics in the synthetic jets' actuating process. This understanding will also be needed for developing the control strategies. As indicated in [5], in most laboratory demonstrations, the SJAs are either too big or too weak. The challenge is to develop an actuator that is not only small, light, robust and economic, but also capable to reach the control objectives. One way to do this is to use the instability of the base flow to enhance the actuation which is decided by the controller [12,19]. In the case of controlling laminar separation using SJAs, the actuation is to use the synthetic jet to *trigger* flow instability. This triggered flow instability may be originally weak but can be enhanced by the instability of the base flow when the generated instability is at the right

frequency, until it becomes substantially strong and effective to meet the control purpose. Based on a numerical investigation, it was claimed that a new instability mechanism was identified which amplified small-amplitude 3-D disturbances in the reattachment zone when the separation bubble was large enough [18]. Work reported in this paper aims to understand this instability enhancement which is essential for developing a micro SJA.

Experimental setup

The experiments were performed in the low speed wind tunnel in the Aerodynamics Laboratory at the University of Technology, Sydney. As shown in Figure 1, in the working section, a fairing was set above a flat aluminum plate with its angle adjustable for establishing the desired pressure gradient, similar to that of a diffusion compressor blade. The flat plate, located 1200 mm from the working section entrance, has a high quality surface finish. The leading edge of the upper surface is of slender elliptical form and the plate has a 0.25^0 negative incidence to avoid leading edge separation.

The SJA used in present study consists of a membrane located at the bottom of a small cavity which has an orifice in the face opposite the membrane. The actuator membrane is a thin circular brass disc, 0.25mm in thickness, held firmly at its perimeter. A piezoceramic disc is bonded to the outside face of the membrane. The lowest resonant frequency of the membrane is 900 Hz and its lump sum capacitance is approximately 140 nF. The SJA was installed underneath the flat plate. The orifice open to the boundary layer flow has a diameter of 0.5 mm. Detailed configurations of the SJA are given in [11]. In operation, as shown in Figure 1, the SJA was driven by a sine wave signal

generated by a standard electrical function generator. An air jet is synthesized by oscillatory flow in and out of the cavity through the small orifice open to the boundary layer.

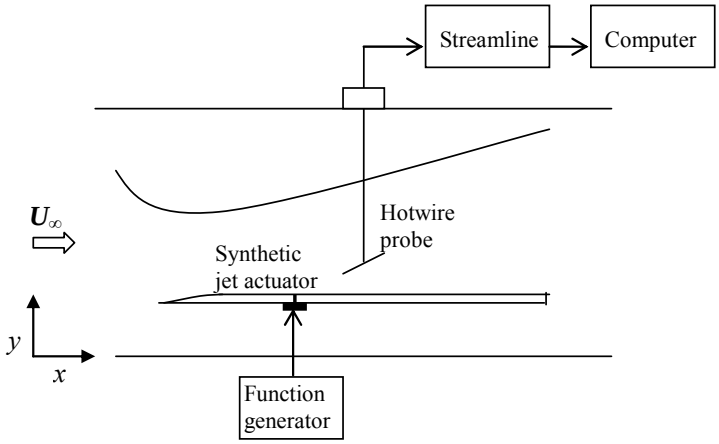

Figure 1 Side view of the experimental setting in the working section

Static taps were located every 25 mm along the streamwise centerline of the flat plate for pressure measurement using a multi-tube manometer. Figure 2 shows the measured pressure distribution. X_0 is the distance from the leading edge of the flat plate. C_p is the pressure coefficient. The minimum pressure is at the position X_0 = 0.285 m, and the centerline of the orifice of the SJA is at X_0 = 0.305 m. Hatman and Wang developed a prediction model for distinguishing three separated-flow transition modes, transitional separation, laminar separation-short bubble and laminar separation-long bubble [10]. The first mode involves transition starting upstream of the separation point, and the latter two have the onset of the transition downstream of the separation point by inflexional instability. The separated flow transition in the current study belongs to the second mode, laminar separation-short bubble, as identified later with results in Figures 3 and 4.

The streamwise velocity was measured, using a Dantec hot wire anemometry, in the boundary layer over the upper surface of the flat plate. The Streamline shown in Figure 1 was a package of software and hardware for interfacing between the computer and the hotwire probe and for data acquisition. The probe was traversed in streamwise (x) and normal (y) directions. A dial gage with a least count of 0.01 mm was used to adjust the probe's position in y direction. The reflection of the probe tip, under a concentrated light source, was used for accurate probe positioning. The sample rate was 6 kHz, and the sample size of each realization was 4096. The axial center of the orifice of the SJA was defined as x = 0 mm. Measurements were made at x = 40 - 160 mm downstream of the SJA (X_0 = 345 – 465 mm in Figure 2) at 20mm intervals.

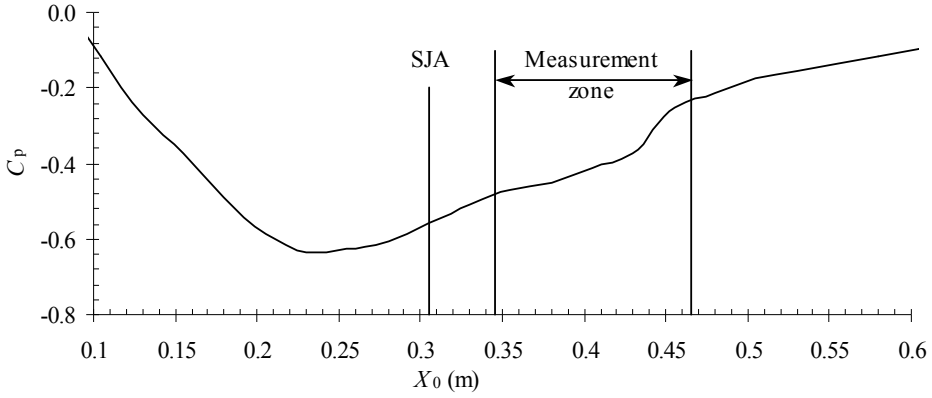

Figure 2 Pressure distribution in the streamwise direction

Effectiveness of synthetic jet actuator

Some coefficients are related to the effectiveness of a SJA. For example, the reduced frequency, $F^+ = f\,(x_c/U_\infty)$. Here f is the forcing frequency, x_c is a characteristic length in the separation region and U_∞ is the local free stream velocity [1,8]. The other one is the momentum coefficient, $C_\mu = h(\rho\, u^2{}_{max})_{jet}/[c(\rho U)_\infty]$, which is defined with the dimensions

of SJA and the maximum jet velocity in the condition without cross flow [8,19]. It was indicated that $C_\mu \geq 0.002$ was necessary before any substantially actuating effects on the flow could be noticed. The effectiveness of the SJA in the present study is identified in terms of the objective of the control system. When the separation bubble disappears due to the actuation of the synthetic jets, the SJA is regarded effective. It does not identify the optimal actuation of the SJA.

Effectiveness of the synthetic jet actuation on resisting the laminar separation was experimentally investigated in our study. Figure 3 shows sample results which demonstrate the effective actuation of the synthetic jets to resist laminar flow separation in a boundary layer with an adverse pressure gradient, by comparing the mean and fluctuating velocity profiles when the SJA was switched on and off. The maximum free-stream velocity, $U_{\infty,\max}$ = 8.0 m/s, was measured at the position with the minimum pressure and at a streamwise position 20 mm upstream of the centerline of the SJA's orifice, x = -20mm. The fluctuating velocity, u', was calculated as

$$u' = \sqrt{\frac{\sum_{1}^{N}(u-\overline{u})^2}{N}}$$

Where u is the instantaneous streamwise velocity, $\overline{u}$ is the mean streamwise velocity, and N is the sample size of one realization. Both the mean velocity and the fluctuating velocity were normalized by $U_{\infty,\max}$. The forcing amplitude was ±7.5Volts and the forcing frequency was 100 Hz. Here the forcing frequency is the frequency of the sine wave generated by the function generator for driving the SJA, and forcing amplitude is the

maximum amplitude of the sine wave. Table 1 provides the distance from the center of the orifice of the SJA to the measurement station as numbered in Figure 3.

Table 1 Distance between the jet and the measurement station

Number of measurement station in x direction	1	2	3	4	5	6	7
Distance to the jet (mm)	40	60	80	100	120	140	160

The mean velocity profiles in Figure 3(a) show how the SJA works to resist the flow separation, while the fluctuating velocity profiles in Figure 3(b) show why. In the condition with the jet off, at the x positions from 60 mm to 120mm, the mean velocity profile at small y/δ position is quite 'normal' to the wall, and the velocity profile has an inflection point. The separation point is located between x = 40 mm and x = 60 mm, and this separation continues to a position between x = 120 mm and x = 140 mm. The fluctuating velocity profiles with jet off show that the separation is laminar and the transition occurs at about the center point of the separation bubble, which is between x = 100 mm and x = 120 mm. Following a short transition, the reattachment of the separation bubble occurs at a position between x = 120 mm and x = 140 mm.

In the conditions with the synthetic jet on, the inflexion points on the mean velocity profiles disappeared. This is due to that the transition occurs at a position before the natural separation point in the base flow, as shown in Figure 3(b). At x = 40 mm, although the mean velocity profile is not significantly modified yet, the fluctuating velocity has been generated by the synthetic jet actuation at y/δ = 0.07 ~ 3.4. The fluctuating velocity increases in both streamwise (x) and normal (y) directions until it

reaches the position of x = 100 mm which is close to the natural transition point of the base flow, as identified later with Figure 5. After that, the fluctuating velocity decreases downstream. It is worth to note that at x = 160 mm, the mean velocity profile with the jet on is 'fuller' than that with the jet off, but the corresponding fluctuating velocity with the jet on is less than that with the jet off.

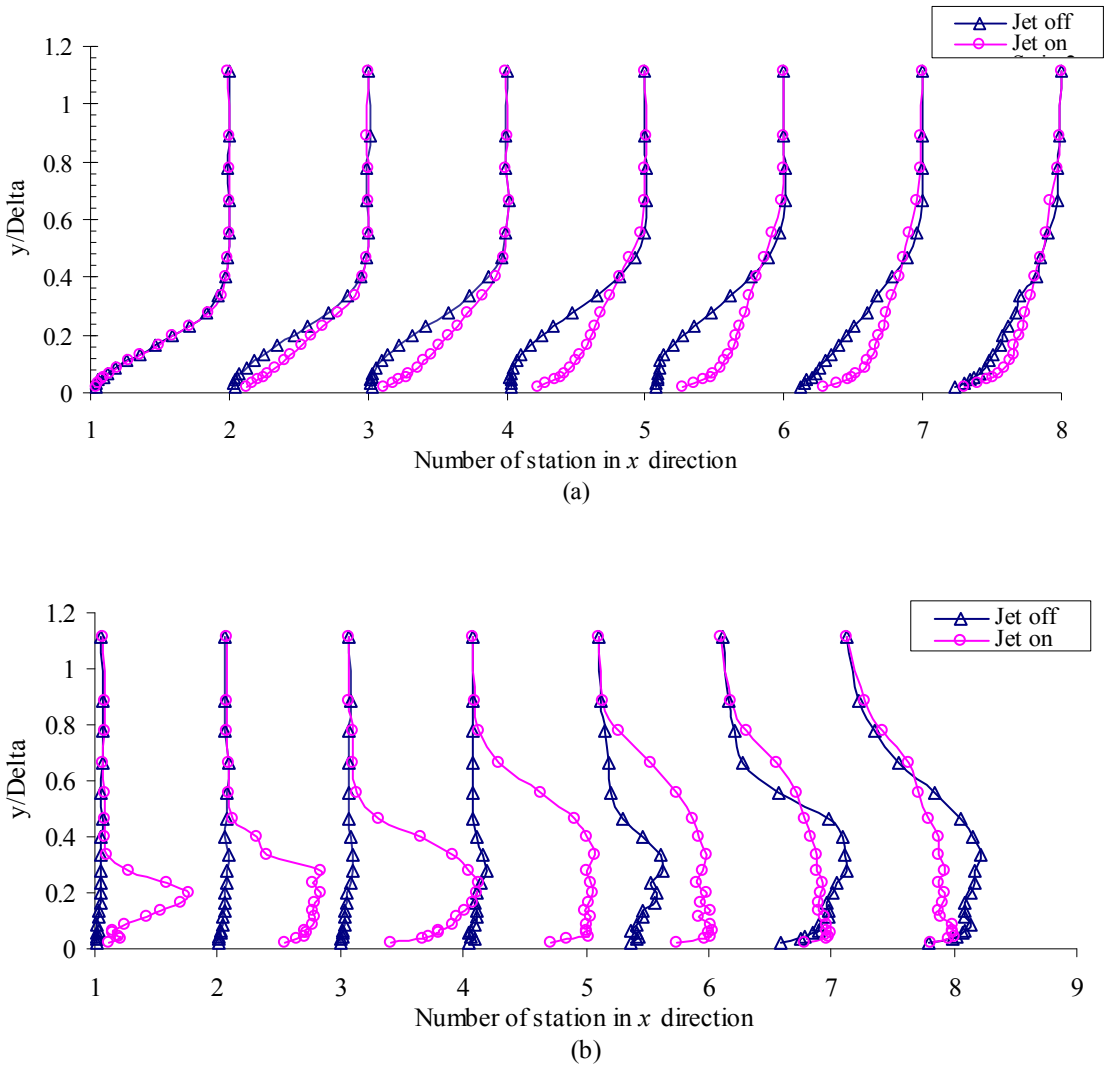

Figure 3 Comparison of experimental results when the jet actuator is switched on and off. (a) Normalized mean velocity profiles and (b) Normalized fluctuating velocity profiles. Forcing amplitude = ±7.5 V., Forcing frequency = 100 Hz. See Table 1 for measurement positions in x direction.

The effectiveness of the synthetic jet on resisting flow separation can also be identified with the displacement thickness. According to the identification methods developed by Hatman and Wang [10], in laminar separation, the maximum displacement of the shear layer occurs at the onset of the transition, and the maximum turbulence level occurs at the first reattachment point. The boundary layer condition in the current study belongs to the laminar separation-short bubble. Figure 4(a) shows the comparison of displacement thicknesses in the conditions with the synthetic jet on and off. As shown in Figure 4(a), the maximum displacement is at about x = 115mm downstream of the SJA when the jet is off. According to the identification method in [10], this position with the maximum displacement thickness should be the onset of the transition in laminar separation. This maximum displacement point is not obvious when the SJA is in operation, as the transition mode has been changed from laminar separation (non-frictional separation) to frictional transition. It is more difficult to define the maximum turbulence level than to define the maximum displacement at a particular x position. However, the fluctuating velocity at x = 140 mm in Figure 4 may be recognized to be greater than that at other x positions. Therefore, the first reattachment point should be between x = 120 mm and x = 140 mm. Comparison of the corresponding momentum thicknesses in Figure 4(b) shows that the SJA increases the momentum transfer from the external potential flow to the boundary layer, so that the boundary layer flow becomes more capable to support the adverse pressure gradient and not to be unattached from the wall.

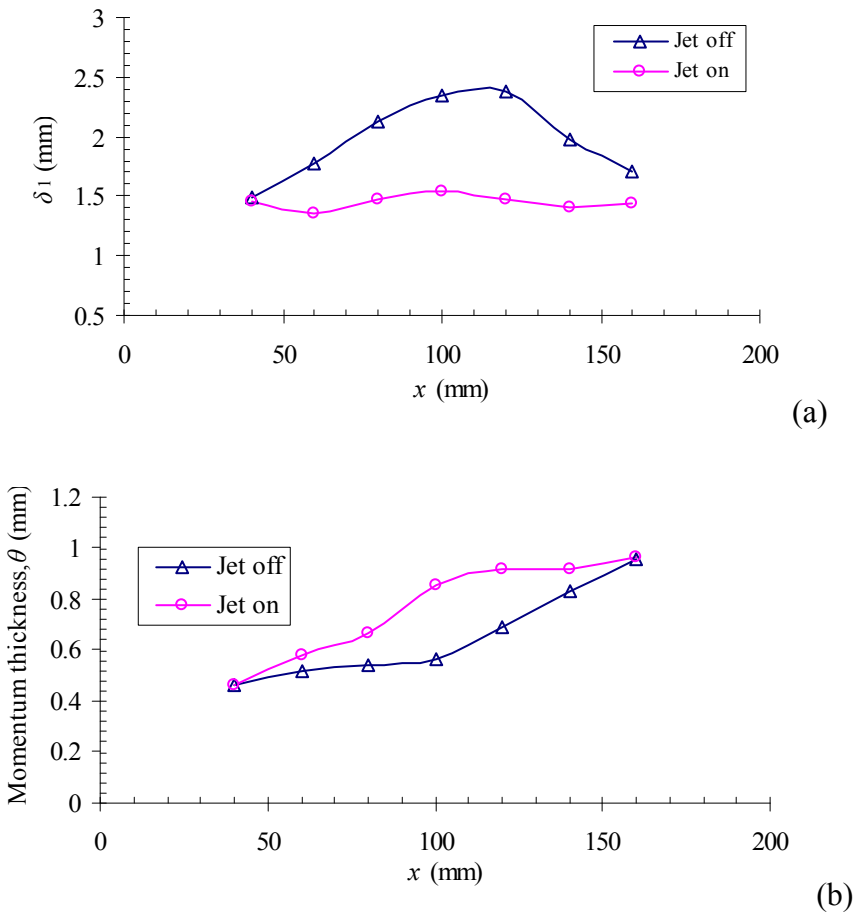

Figure 4 Comparison of boundary layer properties when the jet is on and off

a) Displacement thickness, b) Momentum thickness

Effective forcing frequency

Experimental results in Figure 3 show that the synthetic jets were effective for resisting separation in a boundary layer under an adverse pressure gradient, when the forcing frequency was 100 Hz which was in the frequency range of Tollmien-Schlichting (T-S) instability. However, this effective forcing frequency is different from the most effective forcing frequency, 1.5 kHz, of a synthetic jet actuator when it is operated in a quiescent condition. The most effective forcing frequency in a quiescent condition is defined by the

maximum jet velocity generated at this forcing frequency. 1.5 kHz is the resonant frequency of the membrane material of the SJA [11].

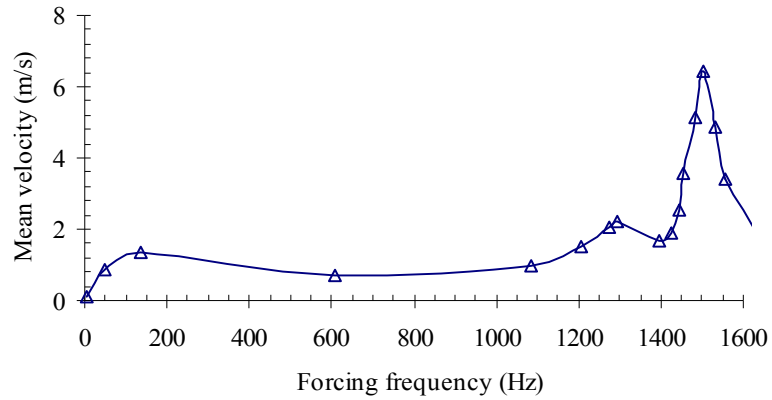

(a)

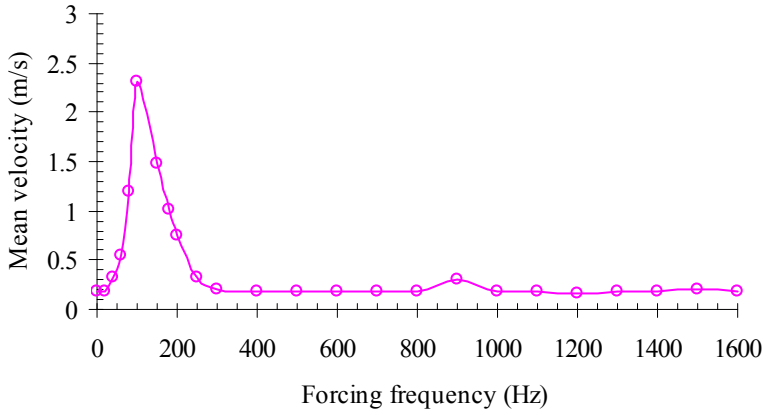

(b)

Figure 5 Mean velocity varied with the forcing frequency
a) without cross flow at y/d = 1.5, b) with cross flow at y/d = 0.8 and x = 100 mm.

Figure 5 shows the variation of the mean velocity with the forcing frequency in the condition with and without crossflow. In the case without crossflow, the velocity was measured at a position y/d = 1.5 along the centerline of the jet. Here d is the diameter of the orifice. y/d = 1.5 was chosen because the maximum mean velocity appeared at this position [11]. The forcing voltage without crossflow was ±7.5V. The peak mean velocity occurs at frequency of 1.5 kHz. In the low frequency bandwidth, a secondary peak

velocity with much smaller amplitude of the mean velocity appears in the range of 100~300 Hz.

In the case with cross flow, as shown in Figure 5(b), the velocity was measured at y = 0.8 mm or y/δ = 0.05 and x = 100 mm downstream of the SJA. This y position was chosen because it was where the maximum fluctuating velocity was detected at the x position which was just upstream of x = 115 mm where the maximum displacement occurred, as identified with Figure 5. Therefore x = 100 mm was the last measurement station to show the effectiveness of the T-S waves triggered by the synthetic jet before the turbulent transition. Compared with Figure 5(a), the mean velocity in Figure 5(b) is significantly greater in the lower frequency range which is the frequency range of T-S waves in the current study. The peak mean velocity occurs at the forcing frequency of 100 Hz. The secondary peak of the mean velocity, which is much smaller, occurs at 900 Hz which is the minimum resonant frequency of the membrane material of the SJA. This shows that, with cross flow, the synthetic jet at lower forcing frequencies is much more effective than that at higher forcing frequencies.

Greenblatt and Wygnanski identified that the optimal reduced frequency, $F^+ = f\,(x_c/U_\infty)$, should be in the order of $O(1)$ for turbulent separation, independently of the turbulence level of the free stream [8]. If this effective reduced frequency is applicable for the control of laminar separation, the x_c needs to be defined if U_∞ is known and f is required to be determined. x_c was defined as the distance from the jet actuator to the tail of the air foil in [5,8]. In the present study, the length of the laminar separation bubble was defined

to be the characteristic length by referring to previous study in [9]. As shown in Figures 3 and 4, the length of the separation bubble was in a range of 60 mm (lower limit) to 100 mm (upper limit). With the measured U_∞, the most effective reduced frequency is in the range of 0.75 (lower limit) and 1.25 (upper limit). If the middle point of the bubble length is taken as the characteristic length, the calculated most effective reduced frequency is 1.0. Although this is consistent with the widely accepted order of the most effective reduced frequency, it should be noted that the effective forcing frequency depends on the condition of the base flow, such as the adverse pressure gradient. As investigated by Walker and Gostelow, the frequency of the T-S waves increased with the increase of the adverse pressure gradient from both the experimental observation and the theoretical calculation. When the characteristic length x_c for calculating the reduced frequency was unchanged (for example, defined by a dimension of an airfoil), significant increase of the adverse pressure gradient (for example, at a poststall angle of attack for an airfoil) should result in high frequencies of the shear layer instability and then lead to the reduced frequency in a higher order than $O(1)$.

It should also be noted that a forcing frequency effective in a condition at low free-stream turbulence may become less effective when the free-stream turbulence is increased. Halfon et al [9] investigated the influence of the free-stream turbulence to the effectiveness of the excitation frequency on reattachment of the separation bubble. Their results showed that the relative reduction in reattachment location decreased as the free-stream turbulence level was increased.

Seifert et al suggested that the most efficient way to trigger any flow instability would be to excite a full spectrum and let the flow select and amplify the most-unstable frequencies and wave numbers [19]. As experienced in our experiments, sharp noise was generated when the SJA was driven in the higher frequency range (800-1600 Hz). Considering the advantage of inaudible noise generated by the SJA driven at lower forcing frequency, the lower T-S instability frequency is more meritorious.

T-S and K-H instabilities

Kelvin-Helmholtz (K-H) instability is known as a non-viscous instability associated with the laminar separation in a boundary layer under adverse pressure gradient, while Tollmien-Schlichting instability is known as a viscous flow instability playing a significant role in the transition at zero pressure gradient. As shown in Figures 3 and identified in Figure 4, the effective actuation of the synthetic jet was realized when the actuator was driven at a T-S frequency. It was believed that the T-S waves, triggered by the synthetic jet and enhanced by the natural instability of the base flow, effectively stopped the flow separation [12]. In the model development for boundary layer separation, Hatman and Wang assumed that the transition to turbulence in separated boundary layer be a result of the superposition of the effects of K-H instability and T-S instability [10]. The fluctuating velocity profiles in the separation zone in Figure 3(b) verify this assumption.

As found in our earlier studies[11], when a synthetic jet was injected in a quiescent condition (without a cross flow), the jet velocity and momentum were maximum at a

forcing frequency which was equal to the resonant frequency of the membrane material of the actuator. However, when the synthetic jet is injected into a boundary layer flow (with a cross flow), whether the disturbance triggered by this small jet is going to be amplified or damped depends on the interaction between the jet and the base flow to be controlled. Why were the T-S waves enhanced rather than damped in our experiments? How did the T-S waves triggered by the synthetic jet interact with the K-H instability of the base flow? The following discussion may lead to or provide some answers.

The potential of closed laminar separation region to act as a generator of disturbance was identified and this identification has been recognized as a significant theoretical development [19]. In a special application of using flapping to control water separation flow in a boundary layer, Rist hypothesized three new mechanisms. One of his hypothesized mechanisms is that a laminar separation bubble itself may act as a resonator with respect to low frequency, long wave length disturbances which should be of the size of the bubble length [18]. Our experimental results positively support this hypothesis. As the length of the separation bubble is in a range of 60 mm to 100 mm. Calculated with the free stream velocity of 8.0 m/s measured at the x position with the minimum pressure, the hypothesized resonating frequency should be in the range of 80 Hz to 133.36 Hz. The forcing frequency for the results of effective synthetic jets shown in Figure 4 was 100 Hz which is within the range of resonating frequency hypothesized by Rist. Therefore, the idea is to use the separation bubble and the associated K-H instability as an amplifier of disturbance whose frequency may be determined by the length of the separation bubble.

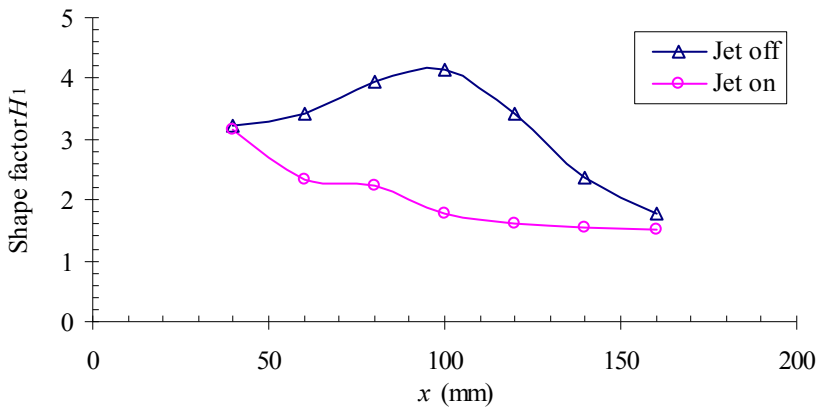

Figure 6 Comparison of shape factors when the jet is on and off

Figure 6 compares the shape factors in the separation bubble region when the synthetic jet was switched on and off, corresponding to the results in Figure 3. In the base flow when the synthetic jet is switched off, the shape factor is increasing and the separation flow is formed until the position of transition. When the synthetic jet is switched on, the shape factor is decreasing and the separation is avoided. Shape factor is interpreted physically as the ratio of the pressure forces to viscous forces. As shown in Figure 6, when this ratio is sufficiently big (> 3) in the case of jet off, the pressure force is significantly greater than the viscous force, so that the viscous force is unable to keep the flow attached to the wall and the K-H instability plays a dominating role in the boundary layer until the transition to turbulence. In this sense, K-H and T-S instabilities compete to each other if both of these two instabilities exist in the boundary layer. However, the K-H instability can also play a role to enhance the T-S instability triggered by synthetic jets. As also shown in Figure 6, in the case of jet on, the adverse pressure gradient and the associated K-H instability provides strong amplification to the T-S waves triggered by the SJA prior to the breakdown to nonlinearity. The amplified T-S waves replaces the

dominating role and reduces the ratio of the pressure force to viscous force to be less than 3, so that the pressure force is not sufficient to separate the flow from the wall.

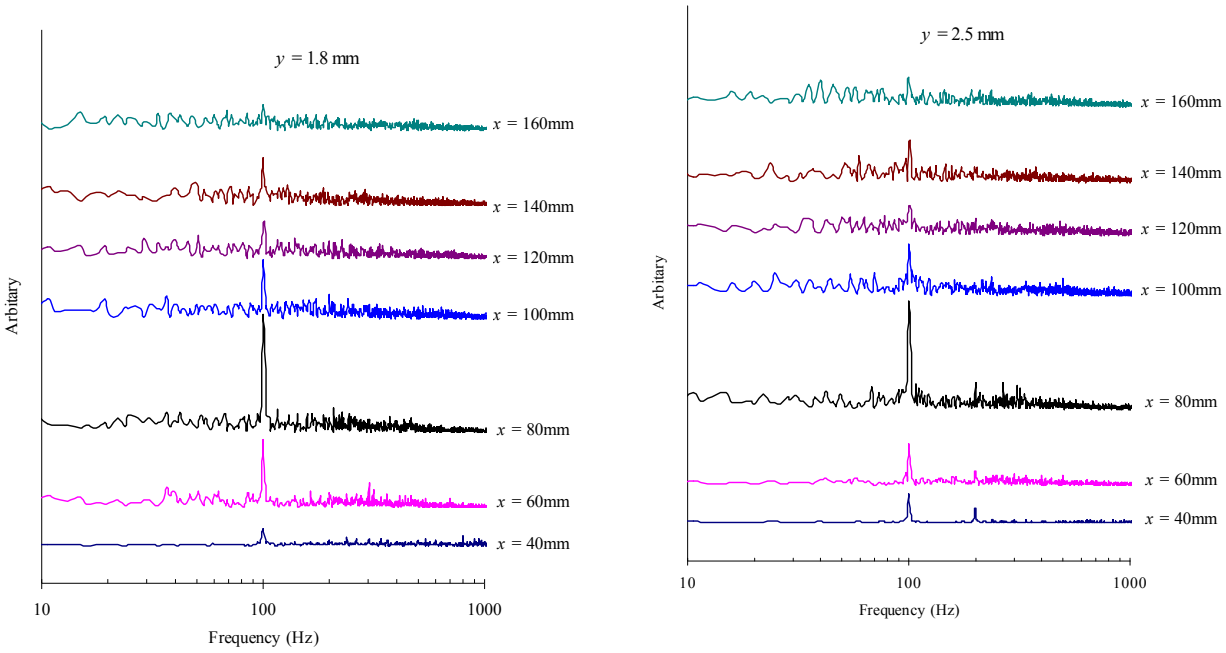

Figure 7 Spectra of instantaneous streamwise velocity at two y positions along the streamwise measurement stations

In Figure 7 are the spectra of the instantaneous velocity measured at the seven streamwise measurement stations at y = 1.8 mm (y/d = 3.6) at y = 2.5mm (y/d = 5.0). The scale of the vertical axis in the graph is arbitrary, but the amplitudes of all the spectra are in the same scale. The peak amplitude of the forcing frequency of 100 Hz retains until x = 140 mm. The amplitude of the frequency component of 100 Hz increases along the streamwise direction and reaches its maximum at a position at x = 80mm, and then decreases to become indistinguishable at x = 140 mm. As identified with the boundary layer properties in Figure 4, the breakdown point, between x = 100mm and x = 120mm, is the onset of the turbulent transition in the laminar separation bubble. This shows that the T-S

waves and the associated linear instability remained to grow and then started to decrease before the flow's breakdown into 3-D non-linear instability. The physics of effective synthetic jet actuation may be hypothesized as follows. A SJA at a low power input triggers 2-D T-S waves. When the T-S waves travel downstream with the base flow in the boundary layer, the T-S waves are amplified by the K-H instability with energy drawn from the base flow. The enhanced T-S waves, in turn, redistribute the drawn energy to perform the required action of resisting separation.

Conclusions

The effectiveness of a SJA on laminar separation control was experimentally investigated. The orifice diameter, which was the characteristic dimension, of the SJA was 0.5 mm. Different methods were applied to identify this control effectiveness. Identification results showed that the synthetic actuator effectively prevented the boundary layer flow from separation caused by adverse pressure gradient. The effective driving voltage was ±7.5 V., and the effective forcing frequency was 100 Hz which was in the range of T-S instability.

The forcing frequency effective for preventing the flow from separation in this experimental investigation was much lower than the most effective forcing frequency, defined by the maximum mean velocity along the centerline of the synthetic jet, in a quiescent (without cross flow) condition. As this most effective forcing frequency in the quiescent condition is equal to the resonant frequency of the membrane material of the synthetic jet, the effective forcing frequency in separation control indicates certain

independency between the control effectiveness and the membrane's material. The lower forcing frequency is preferable as it generates inaudible noise when the forcing power is also sufficiently low. Results also support that the most effective reduced frequency, $F^+ = f\,(x_c/U_\infty)$, should be in the order of $O(1)$. However, the definition of x_c may require caution.

Analysis of the experimental results leads to the conclusion that the flow instability plays an important role in enhancing the effectiveness of the SJAs and also making the effectiveness less dependent of the actuator. The actuation of the SJA is to trigger T-S instability to accelerate the viscous transition. K-H instability dominating the separation boundary layer can become positive in laminar separation control by providing strong amplification to the T-S instability triggered by the SJA. The T-S waves may be initially weak but enhanced by the K-H instability to become substantially strong and effective to meet the control objective. Rather than being used as a generator to provide the "brute force" action, as indicated in [19], the SJA should be used as a trigger to trigger the known instability [8]. This is the key issue in developing an effective micro SJA. Once the actuator actuates, the control effectiveness becomes dependent of the instability characteristics of the boundary layer flow and independent of the actuator's details including the dimensions, weight and structure.

Acknowledgement

The author wishes to acknowledge the experimental work of C. Lee. The advice provided by Prof. J.P. Gostelow and Prof. Y. Fukunishi on T-S instability is gratefully appreciated.

References

[1] Amitay, M. and Glezer, A., "Role of actuation frequency in controlled flow attachment over a stalled airfoil", AIAA Journal, Vol. 40, No. 2, pp. 209-216, February 2002.

[2] Amitay, M., Smith, D., Kibens, V., Parekh, A. and Glezer, A., "Aerodynamic flow control over an unconventional airfoil using synthetic jet actuators" AIAA Journal, Vol. 39, No. 3, pp. 361-370, March 2001.

[3] Cater, J.E. and Soria, J., "The evolution of round zero-net-mass-flux jets", *J. Fluid Mech.*, Vol. 472, pp. 167-200, 2002.

[4] Gad-el-Hak, Mohamed, *Flow Control, Passive, Active and Reactive Flow Management*, Cambridge University Press, 2000.

[5] Gilarranz, J.L., Traub, L.W. and Rediniotis, O.K., "A New Class of Synthetic Jet Actuator – Part I: Design, Fabrication and Bench Top Characterization", ASME J. Fluids Eng., **127**, pp. 367-376, March 2005.

[6] Gilarranz, J.L., Traub, L.W. and Rediniotis, O.K., "A New Class of Synthetic Jet Actuator – Part II: Application to Flow Separation Control", ASME J. Fluids Eng., **127**, pp. 377-387, March 2005.

[7] Glezer, A. and Amitay, M., "Synthetic jets", *Annu. Rev. Fluid Mech*., 34:503-29, 2002.

[8] Greenblatt, D., Wygnanski, I.J., "The control of flow separation by periodic excitation", Process in Aerospace Science, Vol. 36, pp. 487-545, 2000.

[9] Halfon, E., Nishri, B., Seifert, A, Wygnanski, I., "Effects of elevated free-stream turbulence on active control of a separation bubble", AIAA paper 2002-3169, 1st AIAA Flow Control Conference, St Louis, Missouri, USA, 24-26 June 2002.

[10] Hatman, A. and Wang, T., A prediction model for separated-flow transition, ASME Paper, GT-98-237, ASME Turbo Expo '98, Stockholm, Sweden, 1998.

[11] Hong, G., Mallinson, S.G., Lee, C. and Ha, Q.P., On Centerline Distributions Of the Mean Velocity in Synthetic Jets, Proceedings of 14th Australasian Fluid Mechanical Conference, Adelaide, Australia, December 2001.

[12] Hong, G., Lee, C., Ha, Q., Mack, A.N.F., Mallinson, S.G., "Effectiveness of synthetic jets enhanced by instability of Tollmien-Schlichting waves", AIAA paper

2002-2832, 1st AIAA Flow Control Conference, St Louis, Missouri, USA, 24-26 June 2002.

[13] Jenkins, L., Gorton, S. Althoff and Anders, S., "Flow control device evaluation for an internal flow with an adverse pressure gradient", AIAA paper 2002-0266, 2002.

[14] Li, Yong, Ming, Xiao, "Control of two dimensional jets using miniature zero mass flux jets", *Chinese Journal of Aeronautics*. Vol. 13, No. 3, pp. 129-133, August 2000.

[15] Lockerby, D.A., Carpenter, P.W., "Modeling and design of microjet actuators", AIAA Journal, Vol. 42, No. 2, pp. 220-227, February 2004.

[16] Mittal, R. and Rampunggoon, P., "On the virtual aeroshaping effect of synthetic jets", *Physics of Fluids*, Vol. 14, No. 4, April 2002.

[17] Pilon, A., "Aerospace Science", *Aerospace America*, pp13-16, December 2004.

[18] Rist, U., "Instability and transition mechanisms in laminar separation bubbles", VKI/RTO-LS *Low Reynolds Number Aerodynamics on Aircraft including Applications in Emergying UAV Technology*, Rhode-Saint-Gense, Belgium, 24-28 November 2003.

[19] Seifert, A. Theofillis, V., Joslin, R.D., "Issues in active flow control: theory, simulation and experiment", AIAA 2002-3277, 1st AIAA Flow Control Conference, St Louis, Missouri, USA, 24-26 June 2002.

[20] Walker, G.J. and Gostelow, J.P., "Effects of adverse pressure gradient on the nature and length of boundary layer transition", ASME Journal of Turbomachinery, Vol. 122, pp. 196-205, April 1990.